Analytical Methods

RSC Publishing

PAPER

View Article Online
View Journal | View Issue

Cite this: *Anal. Methods*, 2013, **5**, 3497

Polypyrrole nanoribbon based chemiresistive immunosensors for viral plant pathogen detection

Nicha Chartuprayoon,[a] Youngwoo Rheem,[a] James C. K. Ng,[b] Jin Nam,[c] Wilfred Chen[d] and Nosang V. Myung*[a]

Received 7th March 2013
Accepted 18th April 2013

DOI: 10.1039/c3ay40371h

www.rsc.org/methods

Label-free chemiresistive sensors based on a polypyrrole (PPy) nanoribbon (width: 500 nm, thickness: 25–100 nm) were batch-fabricated by a lithographically patterned nanowire electrodeposition (LPNE) technique. A plant pathogen specific antibody was covalently conjugated on the surface of the structure *via* *N*-(3-dimethylaminopropyl)-*N*′-ethylcarbodiimide (EDC)/*N*-hydrosuccinimide (NHS) crosslinking. The sensing performance was investigated by the detection of *cucumber mosaic virus* (CMV). The sensitivity of the nano-immunosensors was enhanced by reducing the electrical conductivity from 1 to 0.005 S cm^{-1} or by decreasing the thickness of the nanoribbon from 100 nm to 25 nm. The reduction in the ionic strength of the pH buffer solutions (*i.e.*, 10 mM PBS to 10 mM PB) also enhanced the sensitivity. However, the reliability and reproducibility of the sensors were significantly reduced by the buffer change. The optimum sensor showed excellent sensitivity with a low and upper detection limit of 10 ng ml^{-1} and 100 μg ml^{-1}, respectively, which is much lower than the low detection limit of traditional enzyme-linked immunosorbent assays (ELISAs) (*i.e.*, 3 μg ml^{-1}).

1 Introduction

Cucumber mosaic virus (CMV), the plant virus genus *Cucumovirus* (family *Bromoviridae*), is commonly found throughout the world and is transmitted by different aphid species to a wide range of vegetable crops including cucumbers, tomatoes, grapes, peanuts, tobaccos, *etc.*[1] Due to its high transmission rate across a wide variety of plants, CMV may cause significant economic losses. However, similar to other plant viruses, effective treatments have not been reported to prevent and/or eliminate CMV infection. Due to the ineffectiveness of chemical treatment, current CMV mitigation strategies mainly involve eradication of infected sources.[2] Therefore, early detection of infection is of the utmost importance and key to the successful management of CMV.

Many serological and molecular detection techniques have been developed and exploited to identify and quantify viral plant pathogens. These include antibody-based assays such as various forms of enzyme-linked immunosorbent assay (ELISA) and electrochemical immunoassay (ECIA), and gene-based real-time PCR.[2–4] Although these techniques can effectively detect viral plant pathogens, they are bound to rigorous laboratory settings, requiring well-trained individuals, costly instruments, and time-consuming processes. Therefore, the development of rapid, accurate, reliable, and miniaturized field-deployable devices for minimally trained personnel is essential.

Among them, one-dimensional (1-D) semiconducting nanostructure-based chemiresistors and/or chemical field effect transistors (ChemFETs) are attractive methods to detect plant pathogens. Owing to their ultra-high surface area to volume ratio, enhanced surface adsorptive capacity, and tunable electrical properties, these label-free electronic biological/chemical sensors have shown to be effective methods to fulfilling the need.[5] Upon binding of bioanalytes on the surface of a nanostructured transducer, such a minute perturbation leads to depletion/accumulation of charge carriers within the bulk of the structure, thus resulting in significant alterations of their electrical properties unlike those of macroscale transducers. This nanostructure-specific feature greatly improves the sensitivity as well as the low detection limit. For this reason, one-dimensional nanostructures including single-walled carbon nanotubes (SWNTs), metal oxide nanowires (NWs), and silicon NWs have been developed for the detection of various biomolecules such as viruses, DNA, proteins, bacteria as well as cells.[5–20] While these studies demonstrated great potential for advancing sensor technology, one of the major challenges is the development of scalable, reproducible and cost effective methods to fabricate and assemble high density devices in large volume.

Despite their short history compared to inorganic materials, conducting polymers such as polypyrrole (PPy), polyaniline

[a]*Department of Chemical and Environmental Engineering, University of California, Riverside, USA. E-mail: myung@engr.ucr.edu; Fax: +1-951-827-5696; Tel: +1-951-827-7710*

[b]*Department of Plant Pathology and Microbiology, University of California, Riverside, USA*

[c]*Department of Bioengineering, University of California, Riverside, USA*

[d]*Department of Chemical Engineering, University of Delaware, Delaware, USA*

(PANI), and poly(3,4-ethylenedioxythiophene) (PEDOT) have emerged as excellent transducers for label-free electronic chemicals/biosensors.[21–27] In addition to their ease of manufacturing nanostructures, diverse monomer chemistries and derivatives of these conducting polymers provide opportunities for simple surface covalent immobilization of antibodies using well-studied bioconjugation chemistry.[28]

Conducting polymer based nanostructured immunosensors demonstrated exceptional sensing performance for detection of biological analytes such as proteins and viruses.[21,28–30] However, the synthesis and packaging of such immunosensors are still a major challenge for mass production. Although various techniques including magnetic[31] and AC dielectrophoretic alignment[21] were attempted to integrate conducting polymer nanowires to the microelectrodes, these methods required tedious and serial processes, which are inappropriate for batch-fabrication of high density sensor arrays.

In this study, we demonstrated the detection of CMV using a chemiresistive immunosensor based on antibody-functionalized PPy nanoribbons. The lithographically patterned nanowire electrodeposition (LPNE) technique was employed to batch-fabricate the PPy sensor by integrating patterned microelectrodes.[32–37] *N*-(3-Dimethylaminopropyl)-*N*′-ethylcarbodiimide (EDC)/*N*-hydrosuccinimide (NHS) was used to surface functionalize antibodies for CMV onto the nanostructured PPy. The sensing performance was optimized by adjusting the electrical conductivity of PPy nanoribbons, the ionic strength of the pH buffer, and the dimensions of the nanostructure.

2 Materials and methods

2.1 Device fabrication and assembly

PPy nanoribbons having a width of 500 nm and thicknesses ranging from 25 to 100 nm were batch-synthesized with integrated gold microelectrodes using the LPNE technique as illustrated in Fig. 1A. The detailed fabrication method is reported elsewhere.[33] Briefly, a sacrificial Ni layer with thicknesses ranging from 25 to 100 nm was e-beam evaporated onto a 4″ thermally oxidized p-type Si wafer (Ultrasil Corporation) with a SiO_2 thickness of 300 nm in step (1). As reported in our earlier work, the thickness of a sacrificial Ni layer dictates the thickness of nanoribbons.[33,35] Sequential spin coating of adhesion promoter P20 (ShinEtsuMicroSi Microelectronic Material, Primer P20) and photoresist (PR) 5214E (AZ Microelectronic Materials, 5214E) was performed at 1000 rpm for 2 s and 3000 rpm for 30 s, respectively. The substrate was baked at 110 °C on a hotplate for 5 min prior to photolithographically defining a pattern by exposing the PR coated substrate to an ultraviolet lamp (applied wavelength of 365 nm with an intensity of 5 mW cm^{-2}) for 7 s. Subsequently, the substrate was immersed in a diluted developing solution (AZ Electronic Materials, 400 K) to develop the pattern. The patterned substrate was dried with ultra-high purity N_2 in step (2). The exposed Ni film was then chemically dissolved by a selective Ni etchant (TFB Transene Company, Inc.), followed by an electrochemical etching of Ni at an applied potential of 0.02 V *vs.* saturated calomel electrode (SCE) in 0.1 M KCl + 24 mM HCl to form a Ni nanoband. Finally,

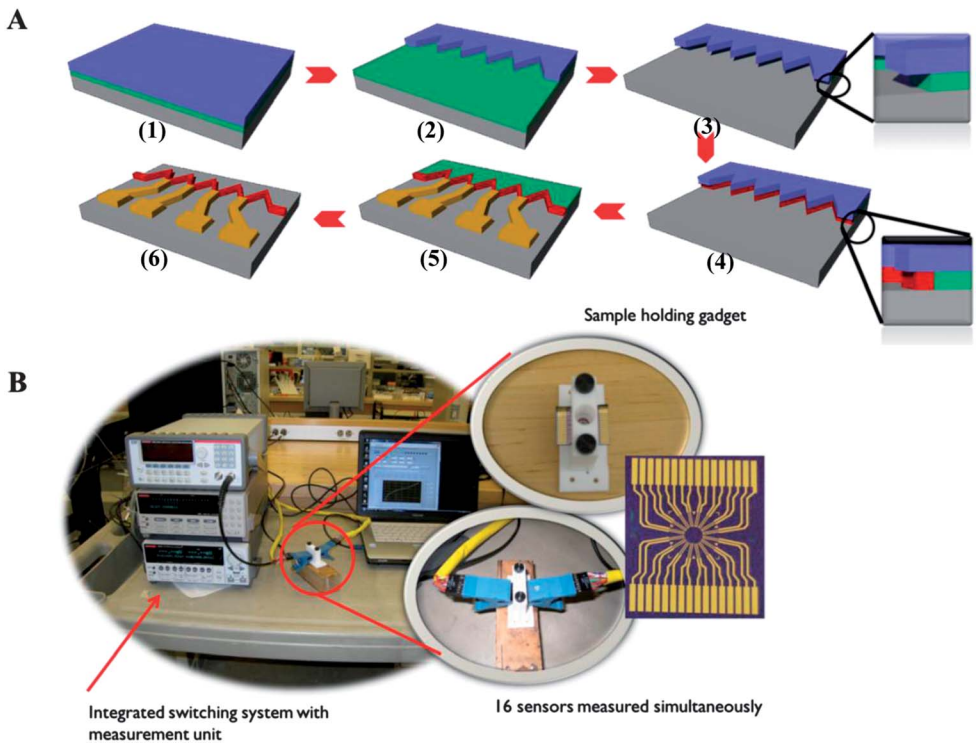

Fig. 1 (A) Schematic illustration of the LPNE process used for the fabrication of PPy nanoribbons, integrated with source and drain microelectrodes. (B) Electrical measurement set-up for biosensing experiment.

PPy nanoribbons were electrochemically synthesized at an applied potential of 0.7 V *vs.* SCE for 4 s at the Ni nanoband in step (4).

After PPy nanoribbon synthesis, the PR layer was removed by soaking the substrate in an acetone bath for 5 min. The same protocol for spin coating of PR and pattern development described earlier was employed to integrate microelectrodes onto the nanoribbons. Ti as an adhesion layer and gold as an electrode material with thicknesses of 20 nm and 180 nm, respectively, were sequentially e-beam evaporated. The substrate was then submerged in an acetone bath to attain patterned microelectrodes in step (5). Excess Ni was selectively removed by 2 v/v% HNO_3 solution, and the sample was dried with high purity N_2 gas in step (6).

2.2 Biofunctionalization of PPy nanoribbons with CMV antibodies and sensing measurement

As shown in Fig. 1B, our method allows fabrication of 16 individually addressable PPy nanoribbons with 3 μm gap microelectrodes at the center of the sample. The device was then mounted on a custom-designed Teflon incubation cell to enclose the area where the PPy nanoribbons were located to improve fluid handling during biofunctionalization and sensing experiments. Electrical measurement was carried out by probing source (S) and drain (D) electrodes using SOIC test clips (Allied Electronics, Texas) connected to a switching system and a sourcemeter (Keithley Instrument 7001 and 2636A, Ohio). The current–voltage (*I–V*) responses of the PPy nanoribbons were obtained by sweeping the voltage from −0.5 to 0.5 V. The electrical resistance of the PPy nanoribbon was determined from the inverted slope of the *I–V* responses between −0.2 and 0.2 V.

For bioconjugation, polyclonal anti-CMV IgG (Agdia, Inc.) was covalently immobilized onto the surface of PPy nanoribbons by using EDC/NHS as a crosslinker.[21] Briefly, the carboxylic acid group of the antibody was activated by EDC/NHS to form an intermediate carboxylate succinimidyl ester, which then chemically reacted to the active amine group of PPy.[21] The PPy nanoribbons were first incubated in a solution which consisted of 20 μl of 40 mM EDC (Sigma-Aldrich) in 0.1 M 2-(*N*-morpholino)ethanesulfonic acid (MES) buffer (pH = 5.5) and 200 μl of 10 mM NHS in dimethylsulfoxide (DMSO) (Thermo Fisher Scientific). After incubation at room temperature for 3 h, the solution mixture was decanted and washed with either 10 mM phosphate buffer saline or 10 mM phosphate buffer at pH 7.4 containing 0.1 v/v% Tween20 and rinsed with the buffer solutions. The washing and rising step was repeated three times. The bioconjugated PPy nanoribbons were incubated with 1 mg ml^{-1} Bovine Serum Albumin (BSA) (Sigma-Aldrich) in the buffer solution for 1 h at room temperature to block non-specific binding. After blocking, the sensors were washed with the Tween20 containing solution and rinsed with the buffer solution three times.

Virions of the Fny strain of CMV, CMV-Fny, were purified from infected *Nicotiana clevelandii* plants by the 'standard' CMV purification procedure previously described.[1] The concentration of purified CMV was estimated at 36 mg ml^{-1} by measuring UV absorption at 260 nm, assuming an extinction coefficient of 5.0 cm^2 mg^{-1}.[38] The CMV stock solution was diluted to 1 mg ml^{-1} aliquots using PBS solution (pH = 7.4). Afterwards, the stock solution was serially further diluted with PBS or PB solution to generate standards having various CMV concentrations ranging from 10 pg ml^{-1} to 100 μg ml^{-1}. The CMV-dependent resistance change of the PPy nanoribbon was measured by incubating 150 μl of solutions containing different concentrations of CMV for 10 min, and washing and rinsing with the buffer solution to remove unbound antigens.

3 Results and discussion

Fig. 2A and B display the fabrication and detection scheme of CMV antibody conjugated PPy nanoribbons along with the corresponding *I–V* characteristics after each step. The electrical resistance is referred to as 'wet resistance' henceforth. The surface functionalization (step 2) of the PPy with CMV antibodies increased the wet resistance by approximately 77%. This may be attributed to the changes in carrier concentration and conformation within the PPy nanoribbons upon covalent immobilization of the bioreceptors.[39] Physical adsorption of BSA (step 3) to prevent non-specific binding further increased the wet resistance of the PPy nanoribbons by 35%. This is likely due to the overall net negative charging of BSA (pI = 4.7) under the working buffer solution.[40] Adsorption of such negatively charged biomolecules on the surface of the p-type semiconductor (*i.e.*, PPy nanoribbons) causes the charge depletion at the interaction zone within the PPy nanoribbon conduction channel.[12] Finally, the virus–antibody binding of CMV (0.1 μg ml^{-1}) to the surface immobilized antibodies further increased the wet resistance of the PPy nanoribbons. Similar to the BSA adsorption, the net negative charges of CMV

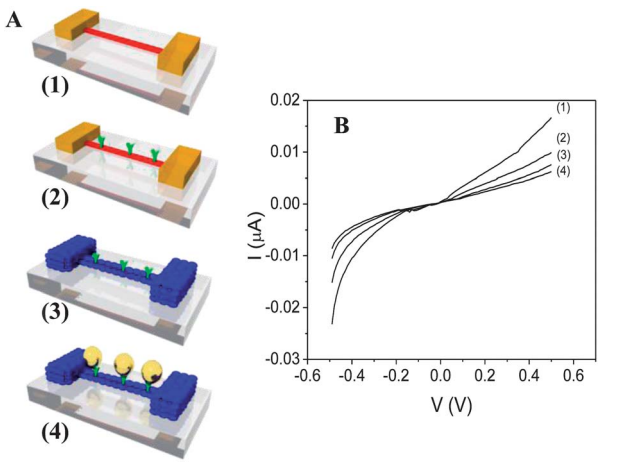

Fig. 2 Schematic representations of the biofunctionalized PPy nanoribbon and the detection of CMV (A) and corresponding *I–V* characteristics after each step: (1) unfunctionalized PPy nanoribbon, (2) CMV antibody functionalized PPy nanoribbon using EDC/NHS chemistry, (3) prevention of non-specific binding by immobilizing BSA onto the nanoribbon, and (4) chemiresistive detection of CMV using PPy nanoribbon.

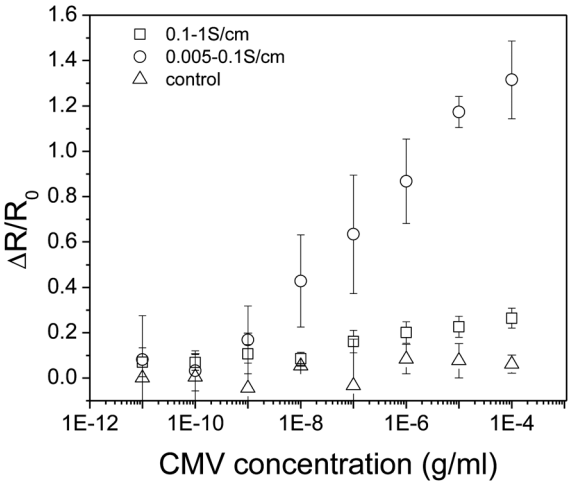

Fig. 3 Calibration plots of resistance change of the immunosensors in various concentrations of CMV with two different ranges of initial conductivity. Non-biofunctionalized PPy nanoribbons were used as a control.

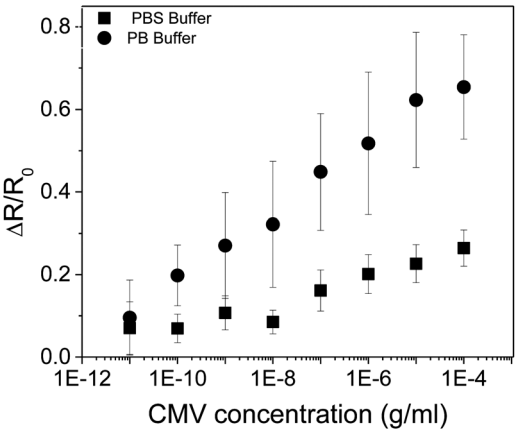

Fig. 4 Calibration plots of resistance change of the immunosensors in various concentrations of CMV in 10 mM phosphate buffer or phosphate buffer saline at pH = 7.4. The electrical conductivities of PPy were 0.1 to 1 S cm^{-1}.

(pI = 4.7) in the buffer solution likely induced a charge transfer to the p-type PPy nanoribbons.[41]

The sensitivity of the anti-CMV functionalized PPy nanoribbon based immunosensor was evaluated by normalized changes in the wet resistance ($\Delta R/R_0$) upon exposure to various CMV concentrations from 10 pg ml^{-1} to 100 μg ml^{-1} in 10 mM PBS buffer solution. To verify that the changes in the measured signals were from specific antibody–virus interaction, *I–V* responses from control samples of PPy nanoribbons (*i.e.*, the nanoribbon without polyclonal CMV antibodies) were assessed. It resulted in a negligible change in the sensitivity ($\Delta R/R_0$) (Fig. 3). After the confirmation of negligible non-specific binding, the CMV sensing experiment was performed using PPy nanoribbons with initial conductivity ranges of 0.1–1 S cm^{-1}. The sensor shows a detection limit of approximately a few μg ml^{-1} and the dynamic range of up to 100 μg ml^{-1}. This detection limit of the nanoribbon based immunosensor is comparable to that of typical ELISA which has been shown to have a detection limit around 3 μg ml^{-1} using a monoclonal antibody as a bioreceptor.[2]

It is reported that a change in the charge depletion/accumulation region, also known as the Debye length (λ_D), causes an alteration of the conductance/resistance within the conduction channel from perturbations due to the adsorption of charged molecules on the surface of 1-D nanostructures.[42] This charge interaction area can be significantly affected by the total charge, temperature, the materials' dielectric constant, and carrier density.[42] Therefore, the change in the conductivity of the PPy nanostructure can result in a charge carrier density change and greatly influence the sensing performance. This was supported by our previous results with PPy nanoribbon based ammonia sensors, in which PPy nanoribbons with lower carrier concentrations produce a smaller conduction channel that enables the flow of electrical charges at the penetration zone.[33] As expected, PPy nanoribbons with lower electrical conductivity (0.005–0.1 S cm^{-1}) enhanced the detection limit to 10 ng ml^{-1} and the overall sensitivity ($\Delta R/R_0$) of the sensor (Fig. 3).

In addition to the Debye screening length within the PPy nanoribbon, the solution Debye length (*i.e.*, electrical double layer in solution), which depends on the ionic strength of solutions (*i.e.*, salt concentration), also affects sensing performance.[18] The elevated salt concentration drastically decreases the solution Debye length, which in turn may inhibit a significant amount of charge transfer from the adsorption of biomolecules to the sensor. Thus, different buffer solutions (*i.e.*, phosphate buffer saline (PBS) and phosphate buffer solutions (PB)) were examined to determine the effects of ionic strength (Fig. 4). The conductivity of the nanoribbon was kept in the range of 0.1–1.0 S cm^{-1}. The sensitivity and low detection limit of PPy nanoribbons in PB buffer were much enhanced than those in PBS buffer. This implies that a larger solution Debye length allows greater charge interaction between molecules and PPy nanoribbons. However, the reliability was decreased in PB buffer showing greater sample to sample variations which may be attributed to the ionic strength dependence of protein and polyelectrolyte interactions.[43]

Another attractive feature of 1-D nanostructure based sensing devices is the ultra-high surface area to volume ratio, which boosts the surface adsorptive capacity. At the same time, the size reduction of nanoribbons can further enhance the sensing performance by making the size closer to the Debye length as shown in Fig. 5.[44] Dimensional changes can be achieved by independently controlling the thickness of the sacrificial layer *via* e-beam evaporation and the width by the duration of electrodeposition in the LPNE process. In this study, the width of the PPy nanoribbons was kept constant at approximately 500 nm, but their thicknesses were varied from 25 nm to 100 nm. Fig. 5 shows the thickness-dependent sensitivity of the sensor. The $\Delta R/R_0$ of 0.29 ± 0.05 at a PPy nanoribbon thickness of 100 nm was improved to 0.72 ± 0.24 at a thickness of 25 nm at a CMV concentration of 1 μg ml^{-1}, but the reduced thickness resulted in greater sensor to sensor variation. This corroborated that the thickness of PPy nanoribbons became a critical parameter to sensitivity tuning.[44]

Overall, the logarithmic dependency of $\Delta R/R_0$ with respect to different CMV concentrations was observed. Nair *et al.*

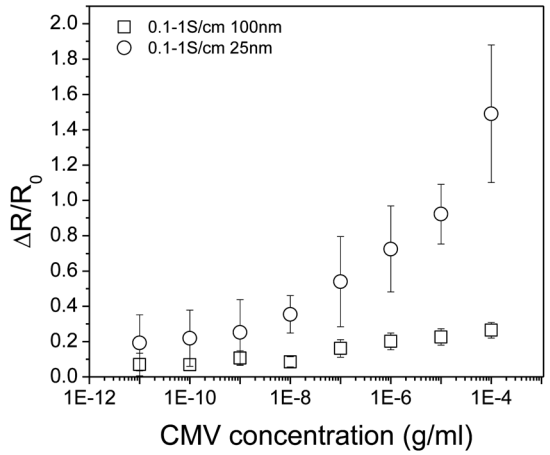

Fig. 5 Calibration plots of resistance change of the immunosensors having different thicknesses of PPy nanoribbons at 25 and 100 nm, in various concentrations of CMV.

explained this logarithmic relationship by the diffusion-capture model and Poisson–Boltzmann equation.[45] The kinetics of the biomolecules adsorbed onto the surface of the biosensors, the mass transfer of biomolecules set by the concentration gradient at the sensor surface, and the rate of molecular interaction between the target analytes and the bioreceptors are governed by the diffusion-capture model.[46] However, the electrostatic screening by dissolved salt solution hampers modulation of the conductance induced by the full charge of the target analytes as shown in Fig. 4. Thus, the Poisson–Boltzmann equation was employed to account for this effect.[44] The sensitivity of biosensors theorized by this model depicted the logarithmic dependency on both the target biomolecule concentration and the ionic concentration. Thus, not only did the sensitivity decrease by increasing the ionic strength, but the longer incubation time was also expected to achieve the same sensitivity.

4 Conclusions

In summary, we have demonstrated the applicability of monolithic PPy nanoribbon based chemiresistive immunosensors for CMV detection. The nanoribbon based sensors showed an excellent sensing performance with low detection limit and a wide dynamic range of up to 100 μg ml^{-1}. The decrease in the electrical conductivity/carrier concentration of the PPy nanoribbon resulted in further improvement of the detection limit down to 10 ng ml^{-1}. In addition, the dimensional reduction in the thickness of the PPy nanoribbon from 100 nm to 25 nm enhanced the sensitivity. Furthermore, the dissolved salt concentration in the buffer solution, which governed the solution Debye length screening effect strongly, affected the biosensing performance. Further investigation of these three factors along with integrated microfluidic channels, selection of monomer chemistries, and their dopants would enhance biosensing performance of conducting polymer based chemiresistive immunosensors.

Acknowledgements

We acknowledge the financial support of grant from the Los Alamos National Laboratory-University of California, Riverside Collaborative Program in Pathogen-Induced Plant Infectious Diseases.

Notes and references

1 J. C. K. Ng and B. W. Falk, *Annu. Rev. Phytopathol.*, 2006, **44**, 183–212.
2 H. S. Zein and K. Miyatake, *Afr. J. Biotechnol.*, 2009, **8**, 751–759.
3 W. Sun, K. Jiao and S. Zhang, *Talanta*, 2001, **55**, 1211–1218.
4 H. S. Zein, J. A. T. da Silva and K. Miyatake, *J. Virol. Methods*, 2009, **162**, 223–230.
5 Y. Cui, Q. Q. Wei, H. K. Park and C. M. Lieber, *Science*, 2001, **293**, 1289–1292.
6 L. N. Cella, W. Chen, N. V. Myung and A. Mulchandani, *J. Am. Chem. Soc.*, 2010, **132**, 5024–5026.
7 L. N. Cella, P. Sanchez, W. W. Zhong, N. V. Myung, W. Chen and A. Mulchandani, *Anal. Chem.*, 2010, **82**, 2042–2047.
8 C. Garcia-Aljaro, L. N. Cella, D. J. Shirale, M. Park, F. J. Munoz, M. V. Yates and A. Mulchandani, *Biosens. Bioelectron.*, 2010, **26**, 1437–1441.
9 F. N. Ishikawa, H. K. Chang, M. Curreli, H. I. Liao, C. A. Olson, P. C. Chen, R. Zhang, R. W. Roberts, R. Sun, R. J. Cote, M. E. Thompson and C. W. Zhou, *ACS Nano*, 2009, **3**, 1219–1224.
10 F. N. Ishikawa, M. Curreli, C. A. Olson, H. I. Liao, R. Sun, R. W. Roberts, R. J. Cote, M. E. Thompson and C. W. Zhou, *ACS Nano*, 2010, **4**, 6914–6922.
11 A. Kim, C. S. Ah, H. Y. Yu, J. H. Yang, I. B. Baek, C. G. Ahn, C. W. Park, M. S. Jun and S. Lee, *Appl. Phys. Lett.*, 2007, **91**, 103901.
12 C. Li, M. Curreli, H. Lin, B. Lei, F. N. Ishikawa, R. Datar, R. J. Cote, M. E. Thompson and C. W. Zhou, *J. Am. Chem. Soc.*, 2005, **127**, 12484–12485.
13 Z. Li, Y. Chen, X. Li, T. I. Kamins, K. Nauka and R. S. Williams, *Nano Lett.*, 2004, **4**, 245–247.
14 K. Maehashi, T. Katsura, K. Kerman, Y. Takamura, K. Matsumoto and E. Tamiya, *Anal. Chem.*, 2007, **79**, 782–787.
15 M. Park, L. N. Cella, W. F. Chen, N. V. Myung and A. Mulchandani, *Biosens. Bioelectron.*, 2010, **26**, 1297–1301.
16 F. Patolsky, G. F. Zheng, O. Hayden, M. Lakadamyali, X. W. Zhuang and C. M. Lieber, *Proc. Natl. Acad. Sci. U. S. A.*, 2004, **101**, 14017–14022.
17 A. Star, E. Tu, J. Niemann, J. C. P. Gabriel, C. S. Joiner and C. Valcke, *Proc. Natl. Acad. Sci. U. S. A.*, 2006, **103**, 921–926.
18 E. Stern, R. Wagner, F. J. Sigworth, R. Breaker, T. M. Fahmy and M. A. Reed, *Nano Lett.*, 2007, **7**, 3405–3409.
19 G. F. Zheng, F. Patolsky, Y. Cui, W. U. Wang and C. M. Lieber, *Nat. Biotechnol.*, 2005, **23**, 1294–1301.
20 G. J. Zhang, L. Zhang, M. J. Huang, Z. H. H. Luo, G. K. I. Tay, E. J. A. Lim, T. G. Kang and Y. Chen, *Sens. Actuators, B*, 2010, **146**, 138–144.

21 M. A. Bangar, D. J. Shirale, W. Chen, N. V. Myung and A. Mulchandani, *Anal. Chem.*, 2009, **81**, 2168–2175.
22 M. A. Bangar, D. J. Shirale, H. J. Purohit, W. Chen, N. V. Myung and A. Mulchandani, *Electroanalysis*, 2011, **23**, 371–379.
23 C. M. Hangarter, M. Bangar, A. Mulchandani and N. V. Myung, *J. Mater. Chem.*, 2010, **20**, 3131–3140.
24 S. C. Hernandez, D. Chaudhuri, W. Chen, N. V. Myung and A. Mulchandani, *Electroanalysis*, 2007, **19**, 2125–2130.
25 K. Krishnamoorthy, R. S. Gokhale, A. Q. Contractor and A. Kumar, *Chem. Commun.*, 2004, 820–821.
26 H. Xie, S. C. Luo and H. H. Yu, *Small*, 2009, **5**, 2611–2617.
27 H.-H. Lu, C.-Y. Lin, T.-C. Hsiao, Y.-Y. Fang, K.-C. Ho, D. Yang, C.-K. Lee, S.-M. Hsu and C.-W. Lin, *Anal. Chim. Acta*, 2009, **640**, 68–74.
28 S. B. Tolani, M. Craig, R. K. DeLong, K. Ghosh and A. K. Wanekaya, *Anal. Bioanal. Chem.*, 2009, **393**, 1225–1231.
29 K. Ramanathan, M. A. Bangar, M. Yun, W. Chen, N. V. Myung and A. Mulchandani, *J. Am. Chem. Soc.*, 2005, **127**, 496–497.
30 D. J. Shirale, M. A. Bangar, M. Park, M. V. Yates, W. Chen, N. V. Myung and A. Mulchandani, *Environ. Sci. Technol.*, 2010, **44**, 9030–9035.
31 M. A. Bangar, C. M. Hangarter, B. Yoo, Y. Rheem, W. Chen, A. Mulchandani and N. V. Myung, *Electroanalysis*, 2009, **21**, 61–67.
32 J. A. Arter, D. K. Taggart, T. M. McIntire, R. M. Penner and G. A. Weiss, *Nano Lett.*, 2010, **10**, 4858–4862.
33 N. Chartuprayoon, C. M. Hangarter, Y. Rheem, H. Jung and N. V. Myung, *J. Phys. Chem. C*, 2010, **114**, 11103–11108.
34 J. E. Hujdic, A. P. Sargisian, J. R. Shao, T. Ye and E. J. Menke, *Nanoscale*, 2011, **3**, 2697–2699.
35 H. Jung, Y. Rheem, N. Chartuprayoon, J. H. Lim, K. H. Lee, B. Yoo, K. J. Lee, Y. H. Choa, P. Wei, J. Shi and N. V. Myung, *J. Mater. Chem.*, 2010, **20**, 9982–9987.
36 E. J. Menke, M. A. Thompson, C. Xiang, L. C. Yang and R. M. Penner, *Nat. Mater.*, 2006, **5**, 914–919.
37 F. Yang, S. C. Kung, M. Cheng, J. C. Hemminger and R. M. Penner, *ACS Nano*, 2010, **4**, 5233–5244.
38 R. I. B. Francki, J. W. Randles, T. C. Chambers and S. B. Wilson, *Virology*, 1966, **28**, 729–741.
39 A. D. Aguilar, E. S. Forzani, X. L. Li, N. J. Tao, L. A. Nagahara, I. Amlani and R. Tsui, *Appl. Phys. Lett.*, 2005, **87**, 193108.
40 Z. G. Peng, K. Hidajat and M. S. Uddin, *J. Colloid Interface Sci.*, 2004, **271**, 277–283.
41 M. H. V. Van Regenmortel, *Virology*, 1967, **31**, 391–396.
42 A. Kolmakov and M. Moskovits, *Annu. Rev. Mater. Res.*, 2004, **34**, 151–180.
43 E. Seyrek, P. L. Dubin, C. Tribet and E. A. Gamble, *Biomolecules*, 2003, **4**, 273–282.
44 N. Elfstrom, A. E. Karlstrom and J. Linnrost, *Nano Lett.*, 2008, **8**, 945–949.
45 P. R. Nair and M. A. Alam, *Nano Lett.*, 2008, **8**, 1281–1285.
46 P. R. Nair and M. A. Alam, *Appl. Phys. Lett.*, 2006, **88**, 233120.

